Highly Ordered Titanyl Phthalocyanine Films Grown by Directional Crystallization on Oriented Poly(Tetrafluoroethylene) Substrate

Martin Brinkmann* and Jean-Claude Wittmann

Institut Charles Sadron, 6 rue Boussingault, 67083 Strasbourg, France

Markus Barthel and Michael Hanack

Universität Tübingen, Institut für Organische Chemie, Tübingen, D72076 Germany

Christian Chaumont

Ecole de Chimie, Polymères et Matériaux de Strasbourg, 23 rue du Loess, 67000 Strasbourg, France

Received September 14, 2001

Highly oriented films of titanyl phthalocyanine (TiOPc) were obtained by high-vacuum sublimation onto an oriented poly(tetrafluoroethylene) (PTFE) substrate. The dependence of the structure and morphology on deposition parameters (substrate temperature T_s, deposition time t, and deposition rate τ) was followed by X-ray diffraction, transmission electron microscopy (TEM), and atomic force microscopy (AFM) to uncover the origin of the oriented growth process. At $T_s = 100$ °C, an original growth mechanism was observed whereby α-TiOPc microcrystallites were formed by the static coalescence and reorganization of small amorphous aggregates in close contact. Nucleation of α-TiOPc is initiated at the PTFE macrosteps from which oriented crystallization propagates, leading to uniform α-TiOPc films with a twinned texture and a dense (0 1 0) contact plane. The molecules are in an edge-on orientation, with their molecular plane oriented parallel to the PTFE chains. At the mesoscale, the nucleation of crystalline α-TiOPc involves the alignment and oriented coalescence of amorphous prenucleation aggregates along the PTFE macrosteps, i.e., a graphoepitaxial process. At the molecular scale, it is proposed that the TiOPc orientation and the preferential nucleation of the α polymorph are enforced by the topography and structure of the PTFE macrosteps in conjunction with the requirement for a minimal nucleation free energy. The optical absorption of the films in the near infrared is found to be strongly correlated with the structural and morphological modifications in the films. The oriented character of the α-TiOPc films results in a strong polarization of the 850-nm band perpendicular to the PTFE chain axis direction.

I. Introduction

Phthalocyanines constitute a unique and versatile class of π-conjugated molecular materials[1] widely used in the dye industry as well as in micro- and optoelectronics for the design of field effect transistors (FETs),[2] organic light-emitting diodes (OLEDs),[3] and gas sensors.[4] Oxometal phthalocyanines (MOPc's) such as vanadyl and titanyl phthalocyanines (VOPc and TiOPc, respectively) exhibit high photoconductivities and interesting nonlinear optical properties,[5] which make these molecules serious candidates for the design of all-organic optical switches.[6] Among the different oxometal phthalocyanines, TiOPc is known as one of the most efficient organic photoconductors in the near-IR and is currently used in laser printers.[7]

In contrast to other phthalocyanines, e.g., CuPc, TiOPc is a nonplanar polar molecule[8] with the titanyl group located perpendicular to the macrocycle, the outer

* Corresponding author. E-mail: brinkman@ics.u-strasbg.fr

(1) (a) Simon, J.; André, J.-J. In *Molecular Semiconductors*; Springer-Verlag; Berlin, 1985. (b) Leznoff, C. C.; Lever, A. B. P. In *Phthalocyanines: Properties and Applications*; VCH Publishers: New York, 1996; Vol. 1-4.

(2) Bao, Z.; Lovinger, A. J.; Dodabalapur, A. *Adv. Mater.* **1997**, *9*, 42.

(3) Friend, R. H.; Gymer, R. W.; Holmes, A. B.; Burroughes, J. H.; Marks, R. N.; Taliani, C.; Dos Santos, D. A.; Brédas, J.-L.; Lögdlund, M.; Salaneck, W. R. *Nature* **1999**, *397*, 121.

(4) Bouvet, M.; Guillaud, G.; Leroy, A.; Maillard, A.; Spirkovitch S.; Tournilhac, F.-G. *Sens. Actuators B* **2001**, *73*, 63.

(5) (a) Henari, F. Z.; Callgham, J.; Blau, W. J.; Haisch, P.; Hanack, M. *Pure Appl. Opt.* **1997**, *6*, 741. (b) Henari, F. Z.; Davey, A.; Blau, W. J.; Haisch, P.; Hanack, M. *J. Porphyrins Phthalocyanines* **1999**, *3*, 331. (c) Dini, D.; Barthel, M.; Hanack, M. *Eur. J. Org. Chem.* **2001**, in press.

(6) Petty, M. C.; Bryce, M. R.; Bloor, D. In *Introduction to Molecular Electronics*; Edward Arnold: London, 1995.

(7) (a) Yamashita, A.; Hayashi, T. *Adv. Mater.* **1996**, *8*, 791. (b) Winter, G.; Heckmann, H.; Haisch, P.; Eberhardt, W.; Hanack, M.; Lüer, L.; Egelhaaf, H.-J.; Oelkrug, D. *J. Am. Chem. Soc.* **1998**, *120*, 11663. (c) Fujimaki, J.; Tadokoro, H.; Oda, Y., Yoshioka, H.; Tomma, T.; Morigushi, H.; Watanabe, K.; Konishita, A.; Hirose, N.; Itami, A.; Ikeuchi, S. *J. Imaging Technol.* **1991**, *17*, 202.

(8) Mizugushi, Z.; Rihs, G.; Karfunkel, H. R. *J. Phys. Chem.* **1995**, *99*, 16217.

10.1021/cm011241o CCC: $22.00
Published on Web 01/11/2002

Table 1. Unit Cell Parameters for Various Polymorphs of Titanyl Phthalocyanine Single Crystals, Powders, and Thin Films

structure	space group	*a* (Å)	*b* (Å)	*c* (Å)	α (°)	*β* (°)	*γ* (°)	*Z*	*V*/*Z* (Å^3)
α-TiOPc (phase II)[8]	*P*-1	12.17	12.58	8.64	96.3	95.0	67.9	2	608
β-TiOPc (phase I)[8,a]	*P*21/*c*	13.41	13.23	13.81	90.0	103.7	90.0	4	595
Y phase[10]	*P*21/*c*	13.85	13.92	15.14	90.0	120.2	90.0	4	630
epitaxial phase[15]	*P*-1	14.0	14.0	10.6	109.2	133.9	90.0	–	–

[a] These unit cell parameters were obtained at $T = 170$ K.

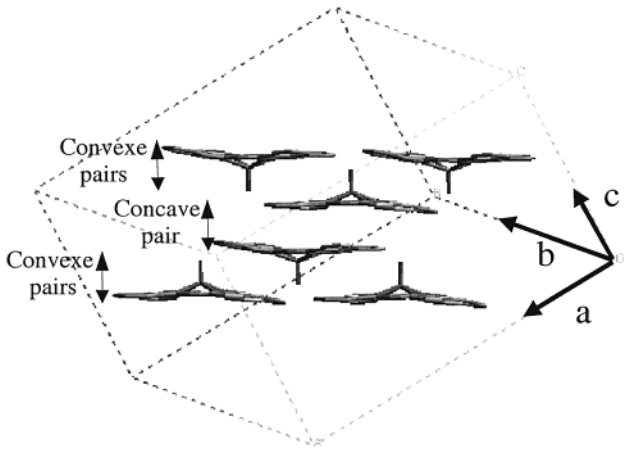

Figure 1. Molecular model of α-TiOPc (phase II) showing the concave and convex pairs.

phenyl rings making an angle of 7° with respect to the C−N inner ring.[9] Both the nonplanarity and the dipolar character of the molecule result in a specific polymorphism that differs significantly from that of planar phthalocyanines. Three crystal structures have been reported so far:[9,10] a monoclinic phase I, a triclinic phase II (hereafter α-TiOPc), and a triclinic phase Y.[8,10] The crystallographic data for these crystal structures are collected in Table 1. In the triclinic α structure (see Figure 1), molecules form concave and convex pairs with very short intermolecular distances ($N_6 \cdots N_6$ distance of around 3.14 Å[8]). Moreover, in α-TiOPc, the geometry of the molecule was found to be strongly distorted with respect to molecules in solution: the molecular symmetry is reduced from C_{4v} to C_1. This molecular distortion was attributed to strong $\pi-\pi$ interactions.[8]

As for planar phthalocyanines, polymorphism governs the crystal packing in thin films and is found to depend strongly on the growth conditions (substrate temperature, deposition rate, and nature of the substrate).[11−14] The optical properties [absorption, photoconductivity, and second harmonic generation (SHG)] turn out to be correlated with the crystal structure of the films.[12,13,15] Thin films of α-TiOPc (phase II) show the largest third-order nonlinear susceptibility ($\chi^3 = 1.7 \times 10^{-10}$ esu).[16]

Previous studies focused on the structure and morphology in TiOPc thin films grown onto substrates such as KBr, ITO glass, and sapphire R(1 −1 0 2).[7,11,14] Even though preferential orientation was observed in the thin films, no long-range in-plane orientation was achieved on the latter substrates. In addition, polymorphism was observed in most cases with the coexistence of phase II and I (α and *β*).[12−14] However, achieving molecular orientation on a large scale is a key issue that can lead to significantly improved charge-transport properties,[17] as well as polarized photoluminescence for instance.[18] In the case of MOPc's, long-range order is expected to affect the relaxation of excitons and hence the ultrafast electronic excitations available for the enhancement of third-order optical nonlinearities. Wittmann and Smith first demonstrated the possibility of orienting various organic systems including polymers and conjugated molecules onto ultrathin crystalline PTFE films obtained by friction transfer.[19] Oriented PTFE substrates have several advantages related to both ease of processability and exceptional nucleating and orienting properties. Various molecular systems of interest for their electroactive properties including sexithiophene (T6),[20] para(nitroaniline),[21] and substituted oligo-paraphenylenevinylenes (o-PPVs)[18] were successfully oriented on this substrate, leading to molecular films with homogeneous orientation over large areas of several square centimeters. In addition, PTFE films are easy to prepare, chemically inert, thermally stable to 300 °C, optically transparent (visible range), and of low cost.

The present study focuses on the growth mechanism of oriented α-TiOPc films deposited onto oriented PTFE substrates and on the effect of structural and morphological modifications on the optical properties of the films. In section II, we summarize the experimental conditions, while section III covers the experimental results concerning the morphology, structure, and optical properties of the thin films. In section IV, we propose a scenario for the thin film growth mechanism.

II. Experimental Section

TiOPc thin films were grown by high-vacuum sublimation using an Edwards Auto306 evaporator system (base pressure of 10^{-7} mbar) from fused quartz crucibles heated by a tungsten filament. The film thickness and depostion rate in the range of 0.2−6.0 nm/min were controlled by using a quartz microbalance. The TiOPc starting material was synthesized by the method proposed by Yao et al.[22] with minor modifications. The

(9) Hiller, W.; Strähle, J.; Kobel, W.; Hanack, M. *Z. Kristallogr.* **1982**, *159*, 173.
(10) (a) Law, K. Y. *Chem. Rev.* **1993**, *93*. 449. (b) Oda, K.; Okada, O.; Nukada, K. *Jpn. J. Appl. Phys.* **1992**, *31*, 2181.
(11) Yonehara, H.; Etori, H.; Engel, M. K.; Tsushima, M.; Ikeda, N.; Ohno, T.; Pac., C. *Chem. Mater.* **2001**, *13*, 1015.
(12) Yamashita, A.; Maruno, T.; Hayashi, T. *J. Phys. Chem.* **1993**, *97*, L4567.
(13) Yamashita, A.; Maruno, T.; Hayashi, T. *J. Phys. Chem.* **1994**, *98*, 12695.
(14) Yanagi, H., Mikami; T.; Tada, H.; Terui, T.; Mashiko, S. *J. Appl. Phys.* **1997**, *81*, 7306.
(15) Yamashita, A.; Matsumoto, S.; Sakata, S.; Hayashi, T.; Kanbara, H. *J. Phys. Chem. B* **1998**, *102*, 5165.
(16) Nalwa, H. S.; Saito, T.; Kakuta, A.; Iwayanagi, T. *J. Phys. Chem.* **1993**, *97*, 10515.
(17) Nakahara, H.; Sun, K. Z..; Fukuda, K.; Azuma, N.; Nishi, H.; Katsube, T. *J. Mater. Chem.* **1995**, *5*, 395.
(18) Gill, R. E.; Hadziioannou, G.; Lang, P.; Garnier, F.; Wittmann, J.-C. *Adv. Mater.* **1997**, *9*, 331.
(19) Wittmann, J.-C.; Smith, P. *Nature* **1991**, *352*, 414.
(20) Lang, P.; Horowitz, G.; Valat, P.; Garnier, F.; Wittmann, J.-C.; Lotz, B. *J. Phys. Chem. B* **1997**, *101*, 8204.
(21) (a) Damman, P.; Dosière, M., Brunel, M.; Wittmann, J.-C. *J. Am. Chem. Soc.* **1997**, *119*, 4633. (b) Vallée, R.; Dosière, M., Toussaere, E.; Zyss. J. *J. Am. Chem. Soc.* **2000**, *122*, 6701.

TiOPc powder was subsequently purified by gradient sublimation. The substrate temperature, in the range of 30−200 °C, was measured at the film surface using a Pt(100) resistance fixed on the substrate surface using silver paste. After deposition, the substrate temperature was rapidly quenched to room temperature (cooling rate of 0.5−1.0 °C/s) using a liquid nitrogen cooling system to prevent modification of the film morphology, e.g., via annealing.

PTFE films were prepared according to a previously described method[19,20] by sliding a PTFE rod at a constant pressure against a glass slide (Corning 2947) held at 300 °C. The crystalline PTFE surface consists of a succession of molecularly flat areas (width of 50−1000 nm) and oriented macrosteps (or terraces) with heights of a few tens of nanometers.[23] The PTFE chains are aligned along the sliding direction. In the analysis of the overlayer/substrate epitaxial relationship, we used the unit cell parameters of the high-temperature phase because crystalline α-TiOPc films are obtained for $T_s \geq 100$ °C. The PTFE high-temperature phase is described by a pseudohexagonal unit cell with $a = b = 5.66$ Å, $c = 19.5$ Å and $\alpha = \beta = 90°$, $\gamma = 120°$ and the PTFE surface of the films is a crystallographic *ac* plane.

The film orientation was first investigated by polarized optical microscopy using a Zeiss microscope. For the TEM study, films with thicknesses of 5−50 nm were coated with carbon films, floated off on water, and then transferred onto copper microscope grids. The films were studied in bright field and diffraction modes with a 120-kV Philips CM12 electron microscope. Tapping mode AFM was performed on a Nanoscope III instrument using Si_3N_4 cantilevers oscillating at a frequency in the range of 250−300 kHz. X-ray diffraction was performed on a Siemens D5000 diffractometer in (θ, 2θ) mode using Cu Kα radiation ($\lambda = 1.54$ Å). UV−vis−near-IR absorption of the thin films (300−900 nm) was measured on a Shimadzu UV-2101PC spectrometer with polarized incident light. The film orientation with respect to the incident light was controlled by mean of a goniometer: 0° orientation is obtained when the incident beam polarization is parallel to the PTFE sliding direction (*c* axis). The crystal structure and diffraction patterns were generated with the appropriate modules of the Cerius[2] program (Molecular Simulations, Waltham, MA).

III. Results

III.1. Effect of Substrate Temperature on Morphology. In Figure 2, we depict the evolution of the thin film morphology probed by AFM as a function of increasing T_s in the range of 75−200 °C for films with thicknesses of 40−50 nm.

For $T_s = 75$ °C, the films consist of a dense packing of small grains (mean radius around 35 nm) completely covering the PTFE substrate. The PTFE macrosteps are decorated by larger grains whose shape reflects that of the crystalline TiOPc phase. This observation, in line with the ED and optical data (see below), suggests that TiOPc films grown at $T_s < 75$ °C onto oriented PTFE consist of an amorphous-like material (hereafter a-TiOPc) with a few microcrystallites localized at the PTFE macrosteps. The grain size distribution is rather broad and suggests that coarsening has already occurred during growth. The shape of the distribution (not shown) is clearly distinct from that observed in systems undergoing Ostwald ripening, which suggests that coarsening is mainly due to grain coalescence during growth.[24]

For $T_s = 85$ °C (Figure 2), two type of grains are observed: (i) small spherically shaped aggregates of

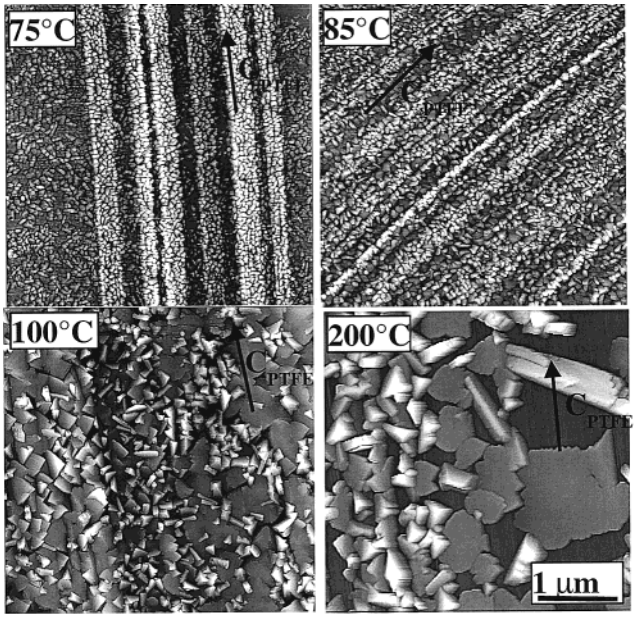

Figure 2. Evolution of the film morphology probed by AFM in TiOPc thin films of thickness in the range of 40−50 nm grown onto an oriented PTFE substrate. Films were obtained at different substrate temperatures in the range of 75−200 °C at a constant deposition rate of 0.8−1.0 nm/min.

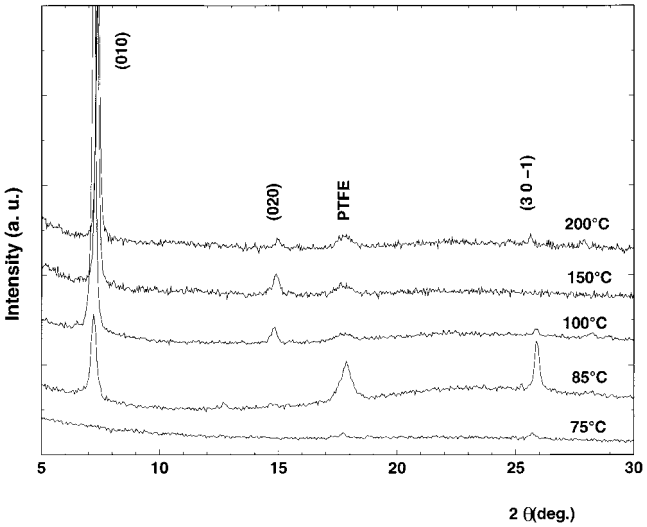

Figure 3. Evolution of the X-ray diffractogram of 40−50-nm TiOPc films grown onto oriented PTFE as a function of increasing T_s (75−200 °C). The diffractograms are shifted along the intensity axis for sake of clarity.

radius <40 nm and (ii) larger crystalline domains of size 50−150 nm with a wedge-like shape. The majority of the crystalline domains are not preferentially oriented on the PTFE, in agreement with the X-ray data (see Figure 3) which provides evidence for different contact planes for α-TiOPc. Similarly to the observations for $T_s = 75$ °C, the larger crystalline domains are located along the PTFE macrosteps. A closer examination of the film morphology reveals that the larger crystalline domains do not have flat surfaces but are composed by smaller aggregates that have coalesced. The preferential loca-

(22) Yao, J.; Yonehara, H.; Pac, C. *Bull. Chem. Soc. Jpn.* **1995**, *68*, 1001.

(23) Fenwick, D.; Smith, P.; Wittmann, J. C. *J. Mater. Sci.* **1996**, *31*, 128.

(24) Zinke-Almang, M.; Feldman, L. C.; Grabow, M. H. *Surf. Sci. Rep.* **1992**, *16*, 377.

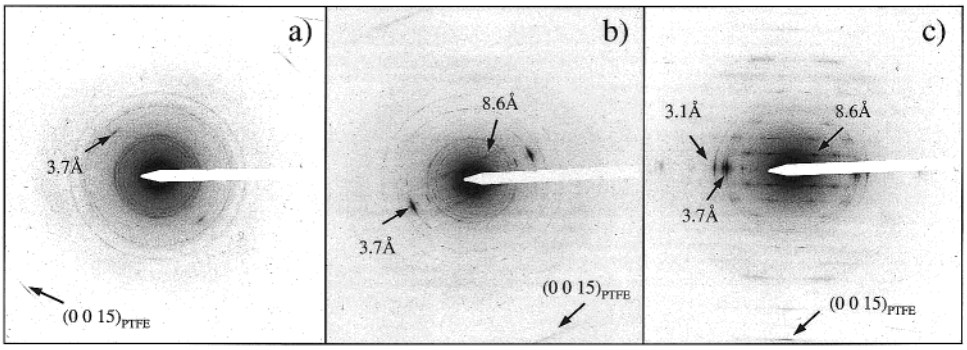

Figure 4. Electron diffraction patterns for TiOPc thin films grown at various substrate temperatures (film thickness in the range of 40−50 nm): (a) T_s = 75 °C, (b) T_s = 85 °C, and (c) T_s = 100 °C.

tion of the larger crystalline domains along PTFE terraces suggests that nucleation of α-TiOPc is heterogeneous.

The morphology is found to change drastically around T_s = 100 °C. The films show a continuous (coverage close to 100%) and polycrystalline texture consisting of large trapezoidal crystallites. The ratio of the film thickness to the in-plane size of the microcrystallites lies in the range of 0.1−0.3. This indicates that the platelet-shaped microcrystallites lie flat on the PTFE substrate. Well-oriented pyramidal-like microcrystallites protrude on the surface of the uniform textured film. These crystallites likely correspond to secondary nuclei grown in a homoepitaxial manner on the underlying TiOPc film. The absence of depletion zones around existing crystallites in conjunction with the continuous film texture suggests again that growth is not driven by Ostwald ripening.

Increasing T_s to 200 °C results in a loss of uniformity in the surface coverage, which decreases to approximately 60−75%. The grains show a variety of shapes and orientations. Admist a majority of flat-lying crystallites, a few crystallites are in an edge-on orientation and are seen by TEM as darker needle-shaped crystals. The latter observation is indicative of a progressive loss of preferential orientation with increasing T_s, in agreement with the appearance of additional diffraction spots in the ED pattern. The decrease of the surface density of microcrystallites with increasing T_s is similar to that observed for other organic materials and stems from the activated character of molecular diffusion and nucleation.[25]

III.2. Impact of Substrate Temperature on Crystal Structure and Orientation. *(a) Effect of Substrate Temperature on Crystallinity and Preferential Orientation*. We used X-ray diffraction (XRD) in (θ, 2θ) mode to follow the evolution of the crystalline order perpendicular to the substrate plane with increasing T_s. Figure 3 depicts the sequence of X-ray diffractograms obtained for increasing T_s. As reported for TiOPc films on sapphire, T_s strongly influences the structure of the films.[13] For $T_s \leq$ 75 °C, no clear diffraction peaks are observed, suggesting that the films are amorphous-like. This result is in contrast to most planar phthalocyanines, which show some crystalline order even for $T_s <$ 50 °C.[2] An important structural change is observed around T_s = 85 °C. We observe two peaks of similar intensities corresponding to reticular distances of 12.0 and 3.44 Å. The PTFE substrate gives rise to a peak at d_{100}^{PTFE} = 4.95 Å that overlaps with a sharper peak due to the TiOPc film. For $T_s \geq$ 100 °C, the intensity of the first diffraction peak at 12.0 Å increases substantially, and a second-order peak at 5.97 Å emerges, whereas the 3.44-Å reflection disappears. Increasing further T_s to 200 °C does not significantly alter the XRD pattern, which remains almost identical to that obtained for T_s = 100 °C. Only a slight decrease of d_{010}^{α} from 12.2 to 11.9 Å is observed as T_s increases. A similar dependence of d_{010}^{α} on substrate temperature has been reported for films grown on sapphire R(1 −1 0 2). On the latter substrate, d_{010}^{α} was found to decrease from 12.0 to 11.6 Å for T_s increasing from 50 to 200 °C.[15]

The two reticular distances of 11.9−12.2 and 5.9 Å are closest to d_{010}^{α} = 11.65 Å and d_{020}^{α} = 5.83 Å reported for single crystals of α-TiOPc.[8] The 3.44-Å diffraction peak is assigned to d_{30-1}^{α} = 3.50 Å. Accordingly, in the T_s range of 85−200 °C only the α structure of TiOPc is nucleated on the PTFE substrate. A preferential orientation of this structure is observed for T_s around 100 °C, with a $(0\ 1\ 0)_{TiOPc}$ contact plane that is preserved for T_s up to 200 °C. This finding is in sharp contrast to previous results reported for films grown onto KBr, ITO glass, and sapphire,[11,13,14] providing evidence for the existence of polymorphism for similar deposition conditions.

Globally, these results provide evidence for the following effects of T_s: (i) a structural transformation from amorphous a-TiOPc to crystalline α-TiOPc in a very narrow T_s range around 85 °C, (ii) the emergence of a preferential orientation of α-TiOPc on PTFE with a dense $(0\ 1\ 0)_{TiOPc}$ contact plane, (iii) a significant change in the d_{010}^{α} value with substrate temperature, and (iv) the preferential nucleation of the α-polymorph for T_s in the range of 85−200 °C.

(b) In-Plane Organization of the Films. The azimuthal orientation of the α-TiOPc crystallites in the plane of the PTFE was determined by ED. Figure 4 depicts the ED pattern sequence obtained for increasing T_s, and Table 2 collects the reticular distances of the dominant reflections.

The ED pattern obtained for $T_s <$ 75 °C (Figure 4a) is dominated by scattering due to the presence of titanium in conjunction with the amorphous character of the films. For T_s = 75 °C, a polycrystalline ED pattern with well-defined diffraction rings is observed. In ad-

(25) (a) Biscarini, F.; Zamboni, R.; Samori, P.; Ostoja, P.; Taliani, C. *Phys. Rev. B* **1995**, *52*, 14868. (b) Brinkmann, M.; Biscarini, F.; Taliani, C.; Aiello, I.; Ghedini, M. *Phys. Rev. B* **2000**, *61*, R16339.

Table 2. d_{hkl} Values Obtained from the ED Patterns of TiOPc/PTFE Thin Films of Thickness 50 nm as a Function of Substrate Temperature T_s

T_s (°C)	d_{hkl} reticular distances (Å)								
75	11.8	–	6.70	5.88	5.36	3.71	–	3.16	2.65
85	–	8.65	6.69	5.96	5.44	3.70	–	3.18	2.68
100	–	8.59	–	–	5.15	3.70	3.52	3.14	–
assignment (α-TiOPc)	(0 1 0)	(0 0 1)	(0 1 1)	(0 2 0)	(1 −1 1)	(2 1 −2)	(3 0 −1)	(2 −1 −2)	(4 3 0)

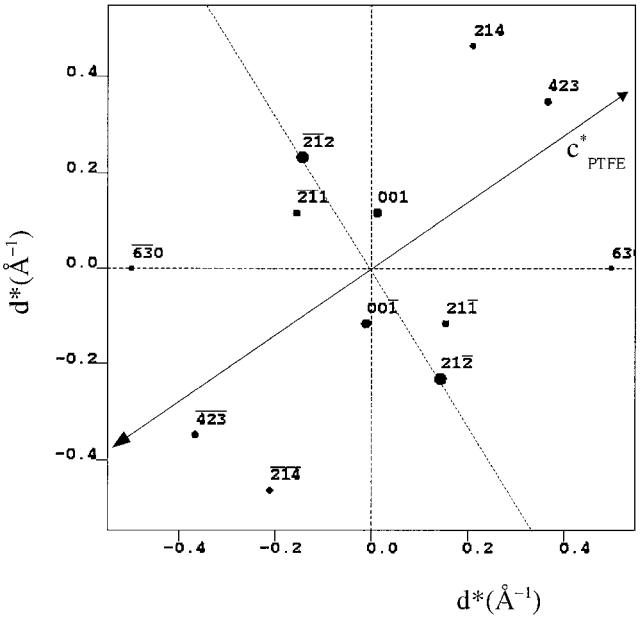

Figure 5. Simulated electron diffraction pattern for an α-TiOPc single-crystal sample with a zone axis [1 −2 0] corresponding to a $(0\ 1\ 0)_{TiOPc}$ contact plane on PTFE.

dition, we observed two arcs oriented along the meridian (with respect to the PTFE c^* axis) that correspond to reticular distances $d^{\alpha}_{010} = 11.8$ Å and $d^{\alpha}_{2-12} = 3.7$ Å. Both of these arcs are oriented in a direction perpendicular to the c_{PTFE} direction, as evidenced by the (0 0 15) reflection at 1.31 Å. This observation suggests the presence of some crystalline α-TiOPc. However, only a small fraction of this crystalline material shows a preferential orientation on the PTFE, in agreement with the XRD and AFM results.

The ED pattern obtained for $T_s = 85$ °C (see Figure 4b) is similar to that observed for $T_s = 75$ °C. However, it differs in two respects: (i) the absence of the arcs at $d^{\alpha}_{010} = 11.8$ Å and (ii) the presence of additional slightly streaked diffraction spots corresponding to $d^{\alpha}_{001} = 8.65$ Å and $d^{\alpha}_{2-12} = 3.70$ Å. The latter diffraction pattern is symmetric with respect to the PTFE chain axis. It indicates the emergence of a preferential in-plane orientation of α-TiOPc.

The ED pattern obtained at $T_s = 100$ °C is typical of a crystalline and fully oriented α-TiOPc film with a twinned texture. The ED pattern in Figure 4c shows two dominant reflections at $d^{\alpha}_{010} = 8.65$ Å and $d^{\alpha}_{-2-12} = 3.70$ Å. To determine the azimuthal orientation of the α-TiOPc microcrystallites in the plane of the PTFE substrate, we simulated the corresponding ED pattern. The simulated ED pattern shown in Figure 5 was obtained for the zone axis [1 −2 0]. It accounts for the dominant (0 0 1) and (−2 −1 2) reflections. The orientation of the electron beam with respect to the α-TiOPc crystal ([1 −2 0] zone axis) corresponds to a $(0\ 1\ 0)_{TiOPc}$ contact plane, consistently with the results obtained from XRD. From Figure 4c, it can be seen that c^*_{PcTiO} is oriented at 53° with respect to c^*_{PTFE}. Given the triclinic structure of α-TiOPc, two orientations of the $(0\ 1\ 0)_{TiOPc}$ contact plane on $(0\ 1\ 0)_{PTFE}$ are possible. Figure 6 depicts the most probable orientation of the $(0\ 1\ 0)_{TiOPc}$ contact plane. TiOPc molecules are in an edge-on orientation, and the plane of the macrocycle is parallel to the PTFE chain axis and is inclined at 116° with respect to the plane of the PTFE substrate (see Figure 6b).

The overlayer/substrate crystallographic relationship obtained from ED and XRD can be summarized as follows

$$(0\ 1\ 0)_{TiOPc}//(010)_{PTFE}$$

and

$$[1\ 0\ -1]_{TiOPc}//[0\ 0\ 1]_{PTFE}$$

Given this overlayer/substrate orientation, no simple relationship between the unit cells of the PTFE substrate and the α-TiOPc overlayer can be found. In particular, the distance between rows of TiOPc molecules parallel to c_{PTFE} (7.36 Å) does not match the interchain periodicity of the PTFE substrate (5.66 Å). Accordingly, a 1D epitaxial mechanism seems unlikely to explain the observed orientation of α-TiOPc on oriented PTFE.

We therefore resorted to 2D coincident epitaxy as a possible mechanism for oriented growth. Coincident 2D epitaxy corresponds to the situation where a fraction of the overlayer lattice points coincide with substrate sites at periodic intervals.[26] This type of epitaxy involves stabilization of the overlayer by favorable interactions at coincident sites, e.g., PTFE grooves between successive chains, which balance the energetic penalty due to noncoincident sites. Analyzing the different possibilities for supercell matching at the $(0\ 1\ 0)_{TiOPc}$ /$(0\ 1\ 0)_{PTFE}$ interface, it can be seen that the supercells needed for commensurate epitaxy typically involve 3−5 unit cells of both substrate and overlayer. Such a situation implies that numerous TiOPc molecules are located on unfavorable sites on the PTFE substrate. In addition, given the lack of long-range order observed along the PTFE chain axis for $T > 50$ °C,[27] 2D coincident epitaxy seems unlikely to explain oriented growth of α-TiOPc. We therefore think that oriented growth of α-PcTiO cannot be simply rationalized on the basis of 1D or 2D epitaxy.

III.3. Growth Kinetics at $T_s = 100$°C. Given the uniformity and high crystallinity of the films obtained at $T_s = 100$ °C, we followed the kinetics of the growth mechanism by depositing films of various thicknesses

(26) Ward, M. D. *Chem. Rev.* **2001**, *101*, 1697.

(27) For $T > 50$ °C, a breakdown of the long-range order along PTFE chains is observed. It results in helical sequences of average length 10 CF_2 units. Kimmig, M.; Strobl, G.; Stühn, B. *Macromolecules* **1994**, *27*, 2481.

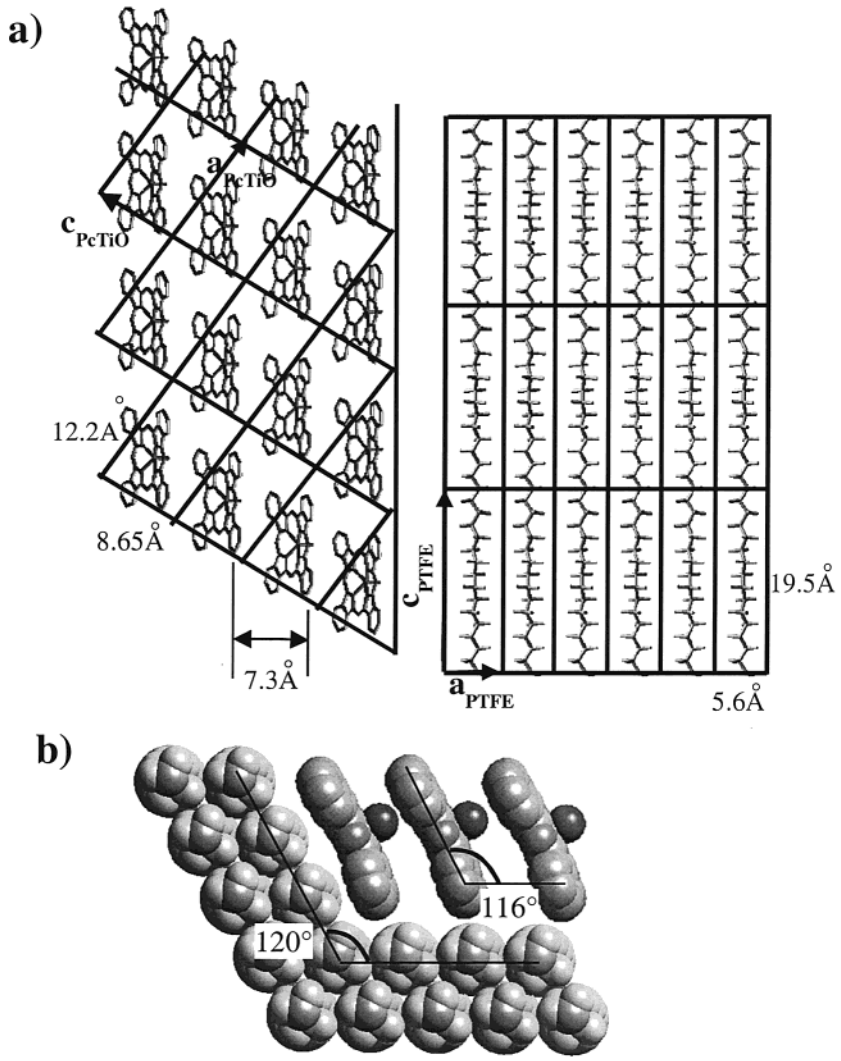

Figure 6. Molecular model of the $(0\ 1\ 0)_{TiOPc}$ contact plane on the oriented substrate of PTFE: (a) Top view of the overlayer and substrate lattices and (b) α-TiOPc/PTFE interface formed at a PTFE ledge between $(0\ 1\ 0)_{PTFE}$ and $(1\ 0\ 0)_{PTFE}$.

h at a constant deposition rate. The evolution of the morphology was subsequently investigated by ex situ AFM. A typical evolution of the film morphology with deposition time (thickness *h*) is depicted in Figure 7.

The morphology is found to change drastically with deposition time. For $h = 1.5$ nm, the PTFE surface is partially covered by small, isolated domains of amorphous TiOPc with a mean diameter <35 nm. Larger domains are observed on top of the flat PTFE macrosteps. No evidence for oriented and crystalline α-TiOPc is found. For $h = 5$ nm, the coverage of the PTFE surface increases, and the films consist of a dense packing of amorphous grains. No important coalescence of the grains is observed. Few crystalline domains are observed at the PTFE macrosteps. A close examination of these crystalline domains reveals a composite structure (see Figure 8); they are formed by spherically shaped grains that have merged to form larger crystalline domains with sharper edges. This observation indicates the heterogeneous character of nucleation and the late-stage character of the orientation mechanism.

The proportion of crystalline domains with respect to amorphous grains clearly increases with increasing film thickness ($h = 10$ nm). Films show alignments of oriented crystallites along the PTFE macrosteps (see Figure 7). For $h = 50$ nm, films are fully crystallized. These observations indicate that the crystallinity in TiOPc films is a function of both increasing T_s and film thickness *h*. The increase of crystallinity with film thickness is qualitatively explained by an annealing process occurring during sublimation and causing a directional crystallization. This growth mechanism is discussed in detail in section IV. Further evidence for such an annealing process during deposition is obtained from the dependence of the film structure on the deposition rate. At elevated deposition rates of 6 nm/min (1 Å/s), the films grown at $T_s = 100$ °C are mainly amorphous-like and appear very similar to those grown at $T_s = 75$ °C at a deposition rate of 0.8 nm/min. These observations demonstrate that crystallization of the films into α-TiOPc is kinetically hindered at elevated deposition rates.

III.4. Optical Properties. *(a) Effect of Substrate Temperature.* In Figure 9, we depict the change in the optical absorption spectrum that accompanies the structural evolution from a-TiOPc to α-TiOPc observed with increasing T_s. The position of the absorption maxima are collected in Table 3. All spectra were recorded for films with thicknesses of 40−50 nm that were oriented with the PTFE chain axis perpendicular to the incident polarized light. The evolution of the absorption spectrum with the polarization of the incident light is depicted in

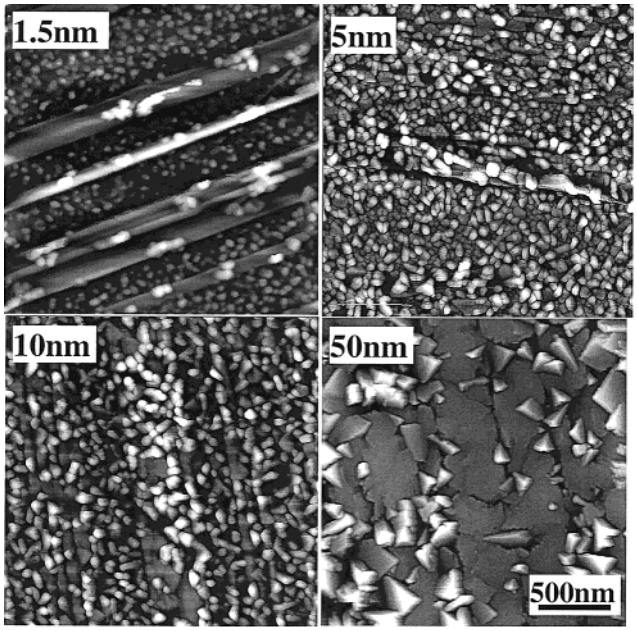

Figure 7. Evolution of the film morphology as a function of increasing film thickness in TiOPc thin films grown onto PTFE at $T_s = 100$ °C (deposition rate $\tau = 0.8-1.0$ nm/min).

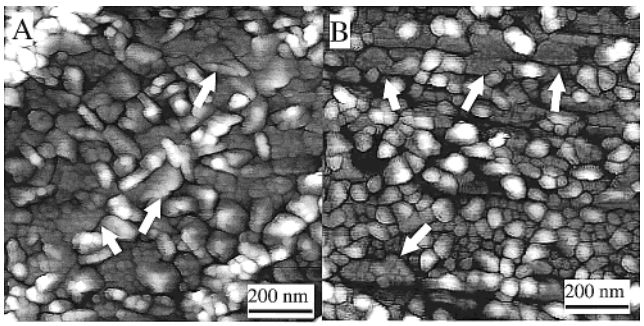

Figure 8. Enlargement of the film topography observed for (a) $T_s = 85$ °C and $h = 30$ nm and (b) $T_s = 100$ °C and $h = 5$ nm. The arrows point to crystalline domains formed by coalescence of amorphous aggregates.

Figure 10a and b for amorphous and crystalline films grown at $T_s = 50$ and 150 °C, respectively.

The structural and morphological transformations described previously coincide with several important changes concerning mainly the Q-band in the range 600−850 nm. The Q-band in the amorphous films obtained for $T_s \leq 50$ °C consists of two overlapping bands with λ_{max} at 666 and 725 nm (see Figure 9). The optical spectrum is found to behave isotropicaly in the substrate plane, i.e., the two bands are not polarized in the PTFE substrate plane (see Figure 10a). The optical absorption observed for $T_s = 75$ °C is similar to that of the amorphous films, but it shows an additional shoulder located around 800 nm. The Soret band in the amorphous films is rather broad and centered around 344 nm, with a shoulder at 370 nm, suggesting the presence of two overlapping components.

Increasing T_s to the onset of crystallization at 85 °C causes a significant change in the Q-band (see Figure 9): the shoulder seen at 800 nm for $T_s = 75$ °C is present as a broad band at $\lambda_{max} = 843$ nm. We attribute the origin of this band to α-TiOPc crystallites nucleated along the PTFE macrosteps. This band is found to be

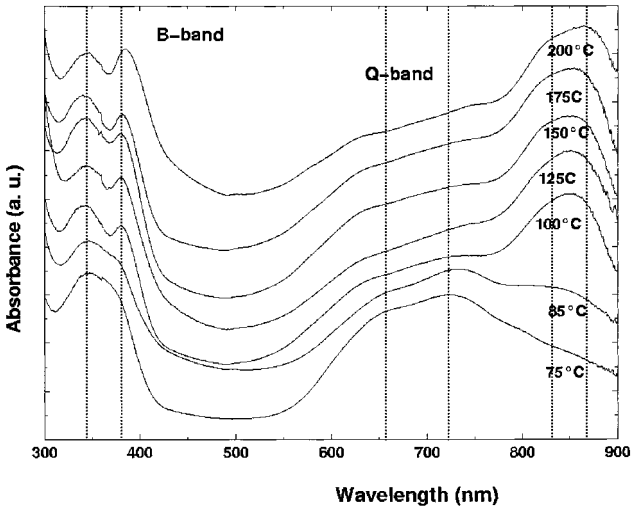

Figure 9. Evolution of the UV−vis−near-IR spectrum as a function of increasing substrate temperature (50−200 °C) for TiOPc films with thicknesses of 40−50 nm. The absorption spectra were recorded with the incident light polarized perpendicular to the c_{PTFE} axis (sliding direction). The spectra were shifted along the absorption axis to clarify the whole figure.

Table 3. Optical Absorption Band Position for TiOPc Films Deposited at Different Substrate Temperatures onto Oriented PTFE Substrate

	λ_{max} (nm)				
T_s (°C)	B-bands		Q-bands		
75	344	371 (sh)	666	725	800 (sh)
85	344	374 (sh)	663	732	843
100	344	378	648	735	854
125	344	379	643	739	855
150	344	380	637	739	855
175	344	383	635	739	855
200	344	385	631	740	859

polarized in the plane of the substrate in a direction perpendicular to the PTFE *c* axis. As for the amorphous films, the two components at 663 and 732 nm are not polarized.

Further increasing T_s results in the following modifications of the optical absorption spectrum (see Table 3): (i) the emergence of a very intense near-IR band that progressively shifts to the red from 843 to 859 nm as T_s increases from 85 to 200 °C, (ii) an increased polarization of the 850-nm band, and (iii) a splitting of the B-band in two components with absorption maxima at 344 and 380 nm, the latter component also showing a redshift with increasing T_s (see Table 3).

For $T_s = 150$ °C (see Figure 10b), both the 380- and 855-nm bands exhibit a significant polarization in the substrate plane. The near-IR absorption band at 855 nm is found to be strongly polarized in the direction perpendicular to the PTFE chain axis. The shape of the near-IR absorption band suggests a composite character, in agreement with results obtained from reflectivity measurements on α-TiOPc single crystals.[8] Similarily to the amorphous films, the two bands at 640 and 740 nm are not polarized in the PTFE substrate plane.

(b) Effect of Film Thickness at $T_s = 100$ °C. The structural transition a-TiOPc → α-TiOPc observed with increasing film thickness *h* at $T_s = 100$ °C coincides with important modifications of the optical absorption spectrum, as seen in Figure 11. The progressive crystalliza-

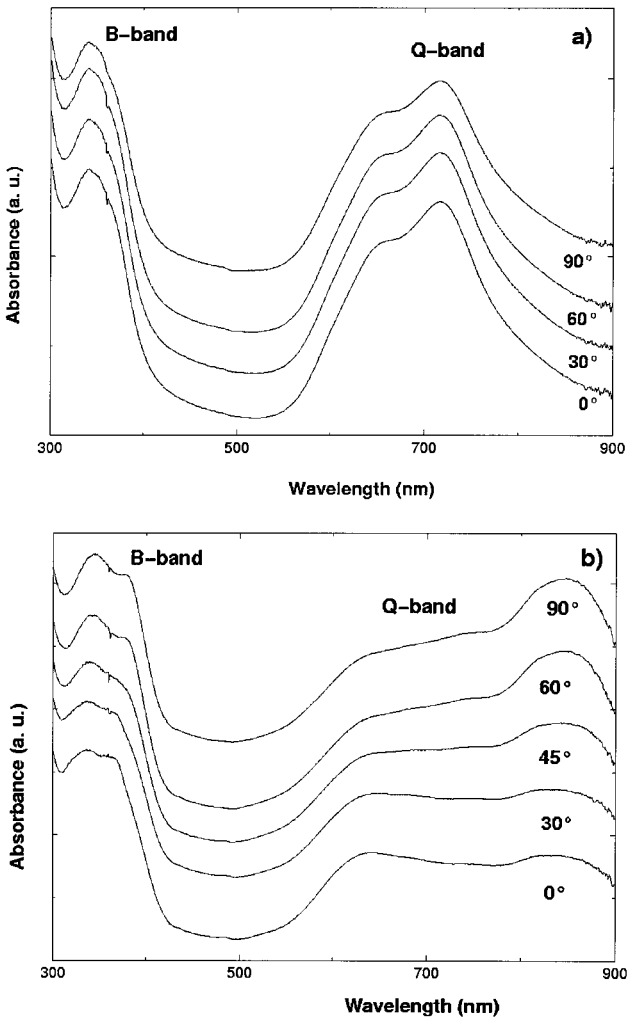

Figure 10. Anisotropy of the UV−vis−near-IR absorption spectrum in (a) amorphous a-TiOPc and (b) crystalline α-TiOPc films grown at $T_s = 50$ and 150 °C, respectively. 0° orientation corresponds to the c_{PTFE} axis (sliding direction) oriented parallel to the polarization of the incident beam.

tion results in (i) the emergence of the near-IR band centered at $\lambda_{max} = 855$ nm with polarization perpendicular to the PTFE *c* axis and (ii) the splitting of the B-band in two components showing maxima in absorbance at 344 and 385 nm. A close look at the absorption spectra of the 1.5- and 5.5-nm films provides evidence of the composite character of the broad band centered at 855 nm. The anisotropy of the latter band is observed for films of thickness $h > 5$ nm. Because this band is attributed to crystalline α-TiOPc, we infer that the small microcrystals seen by AFM for $h = 5$ nm along the PTFE macrosteps are already oriented.

The strong polarization of the near-IR absorption band at 855 nm can be correlated with the molecular orientation of the TiOPc molecules on the PTFE substrate. Indeed, polarized reflectance measurements on α-TiOPc single crystals have shown that the 850-nm band is polarized in the plane perpendicular to the macrocycle, i.e., in the direction of the titanyl group.[8] Our observation for the oriented α-TiOPc films is in agreement with the latter result: the 855-nm band is strongly polarized in the plane perpendicular to the TiOPc macrocycle, i.e., in a direction perpendicular to the PTFE chain axis.

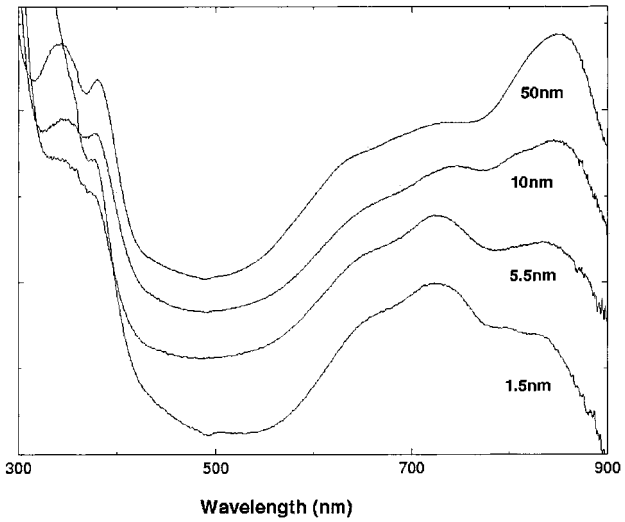

Figure 11. Evolution of the UV−vis−near-IR spectrum as a function of increasing film thickness *h* (1.5−50 nm) for TiOPc thin films grown at $T_s = 100$ °C (deposition rate $\tau = 0.8-1.0$ nm/min). The absorption spectra were recorded with the incident light polarized perpendicular to the PTFE chain axis direction. The optical absorption was normalized with respect to the 50-nm sample and shifted along the corresponding axis to clarify the figure.

IV. Discussion

The growth mechanism of TiOPc on PTFE substrate includes several aspects of interest. In particular, the overall growth kinetics observed at $T_s = 100$ °C can be described in terms of three successive steps: (i) nucleation and growth of amorphous aggregates randomly distributed on the PTFE surface; (ii) heterogeneous nucleation of oriented α-TiOPc nuclei at the PTFE macrosteps via coalescence of amorphous grains; and finally, (iii) directional crystallization from the macrosteps across the PTFE substrate, yielding a uniform α-TiOPc film with a twinned texture.

(i) Formation of Amorphous Prenucleation Aggregates. In the first step, amorphous grains are formed on the PTFE substrate ($h \leq 2$ nm, see Figure 7). The occurrence of the amorphous-like phase for films of thickness <10 nm is attributed to the conjunction of three factors: (i) the dipolar character of TiOPc, (ii) the mechanism and kinetics of the crystallization process, and (iii) a large value of the critical nucleus size for α-TiOPc. Similarly to polar Alq_3, the stability of amorphous TiOPc is attributed to dipolar interactions between TiOPc molecules that add to van der Waals interactions and tend to lock the molecular organization in a random network, favoring the formation of a stable glassy material at sufficiently low T_s.[28,29] Second, it is observed that crystalline α-TiOPc domains are always larger than amorphous prenucleation aggregates. This observation suggests that amorphous grains are more stable (from a thermodynamic point of view) than their crystalline counterpart when their size is below a critical value, which we estimate to lie in the range of 30−40 nm. This proposition is in agreement with the large critical nucleus size r_c determined for many organic crystals. Typical r_c values of a few tens of nanometers

(28) Brinkmann, M.; Gadret, G.; Muccini, M.; Taliani, C.; Masciocchi, N.; Sironi, A. *J. Am. Chem. Soc.* **2000**, *122*, 5147.
(29) Kim, S.-J.; Karis, T. E. *J. Mater. Res.* **1995**, *10*, 2128.

have been reported for organic charge-transfer salts.[30] The occurrence of isolated amorphous nuclei rather than layered crystalline structures during the initial stage of deposition supports a Volmer−Weber island growth mechanism.[26] Such a mechanism is expected when the binding energy in a TiOPc cluster $E_{\mathrm{TiOPc-TiOPc}}$ is significantly larger than the binding energy to the PTFE substrate $E_{\mathrm{TiOPc-PTFE}}$.[26] This situation is similar to that observed for polar Alq_3 deposited onto apolar H-terminated Si(100), where amorphous droplet-shaped domains are formed in the partial wetting regime.[25]

(ii) Nucleation of α-TiOPc at PTFE Macrosteps. In the second step, heterogeneous nucleation of α-TiOPc occurs at the PTFE macrosteps. We consider that the nucleation of oriented crystallites implies two orientational processes occurring at both mesoscopic and molecular scales.

At the mesoscale, the mechanism of nucleus formation is based on the directional coalescence of smaller amorphous aggregates located along the PTFE macrosteps. The preferential nucleation of crystals at macrosteps has been quantitatively demonstrated by Chakraverty and Pound.[31,32] Such a preferential nucleation process involves (i) the preorganization of the amorphous aggregates that are aligned along the PTFE macrosteps and (ii) an important lowering of the free energy of nucleation.

Through condition i, the alignment of amorphous nuclei undoubtedly selects a preferential direction for the coalescence of the amorphous precursor aggregates in addition to a preferential growth direction of the crystal. A significant mobility of the molecules, as well as of the entire aggregates, is required to achieve coalescence and reorganization of the amorphous preagregates into crystalline domains. High translational and rotational aggregate mobilities have been reported for metal clusters with sizes of up to several nanometers and are also likely to be at play in the case of amorphous organic clusters.[31] Both the anisotropy of wetting and the low surface tension of PTFE are likely to control the processes of aggregate mobility and coalescence. Moreover, given the one-dimensional character of the PTFE substrate, molecular diffusion is likely to be highly anisotropic and facilitated in the direction parallel to the PTFE chains.

Condition ii can be understood by considering the expression of the nucleation free energy, ΔG_{nucl}, given in eq 1. The free energy of a nucleus growing on a substrate is determined by (i) the crystallite/substrate interface, (ii) the bulk free energy of the crystal phase, and (iii) the free crystal surface. It can be written as

$$\Delta G_{\mathrm{nucl}} = \sum_{hkl} A_{hkl}\gamma_{hkl} - A_{\mathrm{cs}}\gamma_{\mathrm{cs}} - \Delta G_{\mathrm{c}} \qquad (1)$$

where A_{hkl}, γ_{hkl}, and ΔG_{c} are the area, surface free energy, and free energy associated with the phase change, respectively. The *hkl* and cs indexes refer to the (*h k l*) growing planes and the crystal/surface interface, respectively.

From eq 1, we see that ΔG_{nucl} depends on the amount of new crystal surface created in the nucleation process. When the morphology of the nucleus matches that of the PTFE ledge, a significant reduction of the free energy of the newly created crystal surface occurs. Accordingly, the first term in eq 1, namely, $\Sigma A_{hkl}\gamma_{hkl}$, will be lowered at the expense of the second term $A_{\mathrm{cs}}\gamma_{\mathrm{cs}}$, thereby lowering the global free energy of nucleation. Such a matching of ledge and microcrystallite topologies has been reported for various molecular materials such as benzoic acid and 4-nitroaniline deposited onto organic substrates such as β-succinic acid and L-valine.[33] On the latter substrates, oriented nucleation was found to be controlled by the topography, structure, and lattice parameters of the macrosteps (ledges).

At the molecular scale, a different orientational mechanism is involved. In section III.3, we demonstrated that the TiOPc molecules are oriented with their macrocycles parallel to the PTFE direction. Similarly to the cases of rod-shaped sexithiophene molecules,[20] aromatic *p*-nitroaniniline,[21] and *n*-alkanes,[34] the PTFE substrate is able to select this specific molecular orientation. We propose that the molecular orientation is enforced by both the structure of the PTFE macrosteps and the directional dipolar interactions at the $(0\ 1\ 0)_{\mathrm{TiOPc}}/(0\ 1\ 0)_{\mathrm{PTFE}}$ interface. Despite the apolar character of the PTFE surface, we propose that, on a molecular scale, TiOPc molecules are able to probe the effect of the permanent dipole of the CF_2 units via dipole−dipole and dipole−induced dipole interactions. The CF_2 groups carry a premanent dipole of approximately 2D that is oriented in a plane perpendicular to the PTFE chain axis.[35] Dipole−dipole interactions between CF_2 and polar TiOPc (dipole of 3.7−3.9 D) will be maximized for an "in-line" configuration,[36] which is effectively observed when TiOPc is oriented with its TiO group perpendicular to the PTFE chains.

A possible structure of a PTFE macrostep, albeit not observed directly, is represented in Figure 6b. It is formed by the intersection of two dense and crystallographically equivalent planes, namely, $(0\ 1\ 0)_{\mathrm{PTFE}}$ and $(1\ 0\ 0)_{\mathrm{PTFE}}$, which make a dihedral angle of 120°. As seen in Figure 6b, the dihedral angle between the TiOPc macrocycle plane and the $(0\ 1\ 0)_{\mathrm{TiOPc}}$ contact plane amounts to 116°, whereas the dihedral angle between $(1\ 0\ -1)_{\mathrm{TiOPc}}$ and $(0\ 1\ 0)_{\mathrm{TiOPc}}$ is close to 107°. Accordingly, the molecular orientation of the TiOPc molecule in the $(0\ 1\ 0)_{\mathrm{TiOPc}}$ contact plane matches well the dihedral angle of the PTFE ledge. Concerning the α-TiOPc microcrystals, two dense planes, namely, (0 1 0) and (1 0 −1), can be in contact with the PTFE substrate. This last condition ensures the required minimization of the nucleation free energy ΔG_{nucl} via minimization of the new free crystal area (see eq 1). In addition, the proposed orientation of the TiOPc molecule by PTFE ledges is able to explain the preferential nucleation of the α-polymorph. Indeed, considering the other TiOPc

(30) Molas, S.; Caro, J.; Santiso, J.; Figueras, A.; Fraxedas, J.; Mézière, C.; Fourmigué, M.; Batail, P. *J. Cryst. Growth* **2000**, *218*, 399.
(31) Givargizov, E. I. In *Artificial Epitaxy (Graphoepitaxy)*; Handbook of Crystal Growth Vol. 3; Hurle, D. T. J., Ed.; Elsevier Science: New York, 1994.
(32) Chakraverty, B. K.; Pound, G. M. *Acta Metall.* **1964**, *12*, 851.
(33) (a) Carter, P. W.; Ward, M. D. *J. Am. Chem. Soc.* **1993**, *115*, 11521.
(34) Damman, P.; Fischer, C.; Krüger, J. K. *J. Chem. Phys.* **2001**, *114*, 8196.
(35) *Handbook of Chemistry and Physics*; CRC Press: Boca Raton, FL, 1986; p E59.
(36) Israelachvili, J. A. In *Intermolecular and Surface Forces*; Academic Press: New York, 1992; p 44.

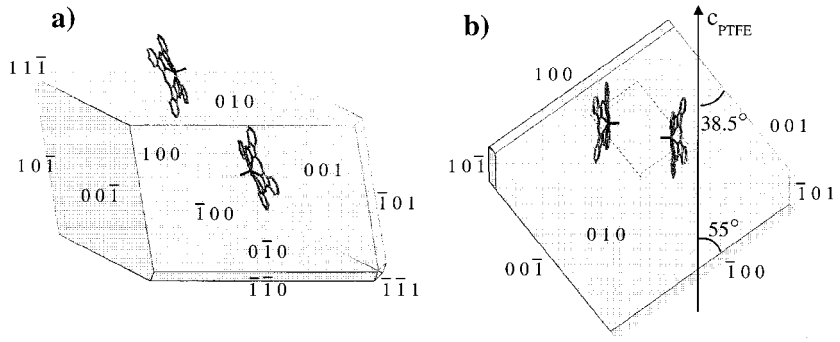

Figure 12. Calculated growth morphology and unit cell orientation within the crystal as calculated by the attachment energy method for α-TiOPc (phase II): (a) side view and (b) top view parallel to the (0 1 0) contact plane of the crystal.

Table 4. Growth Morphology of a α-TiOPc Crystal Calculated by the Attachment Energy Method[a]

crystal face (*h k l*)	D_{hkl} (au)	percent of total crystal area (%)
(0 1 0)/(0 −1 0)	21.7	21.8
(1 0 0)/(−1 0 0)	33.6	12.5
(0 0 1)/(0 0 −1)	37.5	11.8
(1 1 0)/(−1 −1 0)	46.0	1.5
(1 1 −1)/(−1 −1 1)	56.0	0.3

[a] See text.

polymorphs (β and Y), no such favorable matching between molecular orientation and ledge geometry is observed.

(iii) Directional Crystallization. In a process we qualify as directional crystallization, the oriented crystalline nuclei promote crystallization across the whole film surface by reorganization of the TiOPc molecules drawn from the reservoir of amorphous aggregates. Such a growth mechanism can be considered as an annealing process occurring during film deposition. It is known for molecular crystals that crystallization occurs in fast-growth directions. Hartmann and Perdock have demonstrated that the crystal shape is determined by the growth rates of the crystal faces which are proportional to the attachment energies E^{att}_{hkl} of the slices (*h k l*).[37] E^{att}_{hkl} corresponds to the energy release per structural unit as the crystal slice (*h k l*) attaches to the crystal surface from an infinite distance. Simulation of the growth morphology of α-TiOPc crystals was performed using the adapted module of the Cerius[2] program. E^{att}_{hkl} was calculated for suitable slices (*h k l*) selected by the Bravais−Friedel−Donnay−Harker method.[38] From the energy calculation, i.e., the growth rates of the faces, a center-to-face distance D_{hkl} was derived for each face. The resulting morphology is depicted in Figure 12, and Table 4 collects the relative areas of the crystal faces and the D_{hkl} values.

First, we observe that the calculated crystal morphology reproduces well the experimental one. Indeed, the angles between the crystal edges corresponding to the faces (0 0 1) and (−1 0 0) and the PTFE direction match well the experimental values. From Figure 2, we measure angles of ±(38 ± 5)° and ±(58 ± 5)° between the crystal faces and the PTFE chain direction. These values are in excellent agreement with the calculated values of 38.5° and 55°. Second, the calculated crystal morphology provides evidence for a platelet shape (see Figure 12) with an aspect ratio of 2.8 similar to that observed by AFM. The smallest facets, namely, (1 1 −1) and (1 0 −1), correspond to the fast-growth directions, i.e., the directions with the largest attachment energies. The (1 0 −1) direction corresponds to the direction along which intermolecular contacts are most favorable. Indeed, the $N_6\cdots N_6$ intermolecular distance between TiOPc molecules belonging to convex pairs is particularly short (3.145 Å[8]) and lies below the N···N van der Waals distance of 3.45 Å. We therefore expect the strongest van der Waals and dipolar interactions, as well as $\pi-\pi$ overlaps to occur in a direction perpendicular to the molecular plane that coincides almost with the (1 0 −1) plane. In addition, this fast-growth direction is found to be perpendicular to the PTFE chain axis. The truncated trapezoidal shape of the TiOPc crystals observed by AFM and TEM further demonstrates the heterogeneous nucleation of α-TiOPc at the PTFE macrosteps: it arises because crystallization is enforced in a direction perpendicular to the macrostep and away from it.

From Table 4, it can also be concluded that the (0 1 0) and (0 −1 0) crystal facets give the largest contribution to the crystal surface area (43.5%). The fact that these crystal planes correspond to the contact planes is fully consistent with the thermodynamic requirement for a minimal nucleation free energy ΔG_{nucl}. α-TiOPc platelets have a natural tendency to lie flat on the substrate because the amount of additional surface (see eq 1) is minimized in this way.

V. Conclusion

In this study, we have been able to uncover the growth mechanism in oriented TiOPc thin films grown onto PTFE substrates by following the growth kinetics at $T_s = 100$ °C and the dependence of the morphology on the substrate temperature. Rather than epitaxy-based growth (both 1D and 2D) and graphoepitaxy, the growth mechanism observed in the case of TiOPc/PTFE involves orientational processes occurring at both mesoscopic and molecular scales. At $T_s = 100$ °C, oriented growth can be described in terms of three distinct steps: (i) nucleation and growth of amorphous aggregates randomly distributed on the PTFE surface; (ii) heterogeneous nucleation of oriented α-TiOPc nuclei at the PTFE macrosteps via coalescence of amorphous grains; and finally, (iii) directional crystallization of the

(37) Liu, X. Y.; Bennema, P. *J. Cryst. Growth* **1996**, *166*, 117.

(38) Only van der Waals interactions have been used in our calculations, as the Coulombic contribution has been neglected. For further information on the calculation procedure, see the Cerius[2] Users's Guide section on Computational & Analytical Instrumentation, pp 131−143, and references therein.

α structure in a fast-growth direction (1 0 −1) perpendicular to c_{PTFE}, yielding uniform films with a twinned texture. At the mesoscale, the mechanism of nucleus formation is based on the directional coalescence of smaller amorphous aggregates preferentially aligned by the PTFE macrosteps. At the molecular scale, both the orientation of TiOPc and the preferential nucleation of the α polymorph are enforced by the topography and the structure of the PTFE macrosteps. This high molecular orientation achieved for $T_s = 100$ °C results in a strong polarization of the UV−vis−NIR absorption band located at 850 nm.

Acknowledgment. We acknowledge support from EEC Contract ERB FMRXCT 970106. M. Scheer and C. Straupe are acknowledged for technical support. Fruitful discussions with Bernard Lotz are also gratefully acknowledged.

CM011241O